

vegetation (greater than 100%) occur because the spectral contrast between the actual green vegetation in the forested wetland and mixtures of the soil and NPV endmembers is greater than that of the green vegetation endmember used to model the scene. The high shade fraction is also distinctive of the forested wetland. The fractions labeled B in Figure 1 are characteristic of senescent grassland (low shade and high fractions of NPV). This ability to relate spectral fractions to surface composition facilitates a meaningful classification of the scene.

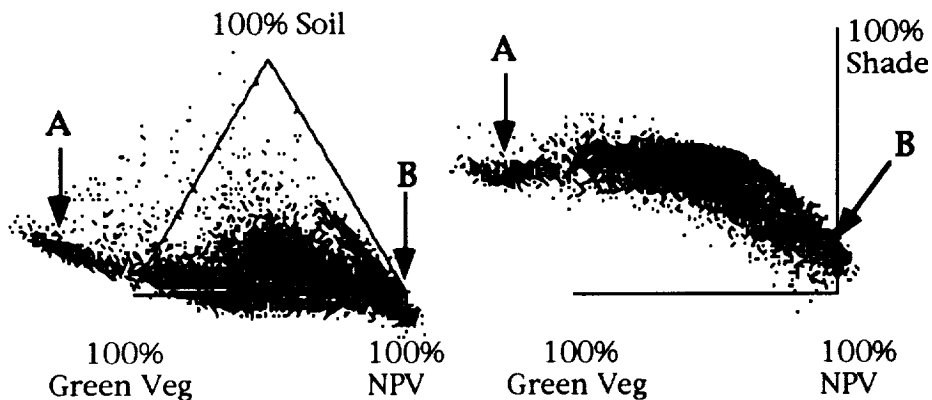


Figure 1: Distribution of fractions for a subset of the June 2, 1992 AVIRIS image of Jasper Ridge. Fractions indicative of the forested wetlands is labeled A and those for the grasslands, B.

The classification scheme is shown in the ternary diagram in Figure 2. Class boundaries in this scheme are linear and may appear arbitrary. In early investigations of this approach to classification, the boundaries were mapped as being slightly curved. It was subsequently determined that linearizing the boundaries simplified application of the classification with little change in the final results. Although not shown in Figure 2, the shade fraction (a relative measure of canopy architecture of plant communities) was used in the classification. For example, pixels containing tall bushes and trees (i.e. forested wetland, chaparral, and deciduous oak woodland) typically contained greater than 35 percent shade at the time of image acquisition.

Images classified using this approach closely matched vegetational maps of the surface. Figure 3 (Slide 11 in the pocket attached to the cover) shows the classified June 2nd image next to a vegetation map (mapped in the field) for comparison. The classes (and colors) are the same for both maps. The degraded grassland, however, was not mapped separately from grassland in the field map, as it was in the classification image.

Preliminary results show that observation of temporal changes in the fractions can be useful in monitoring surface processes. Temporal changes in the fractions of the forested wetland, chaparral, and grasslands are shown in Figure 4. The raw fractions (open symbols) are those calculated from spectral mixture analysis. Most of the vegetation communities had low fractions of soil. Detection-threshold analysis (Sabol et al., 1992a) was used to determine whether the low soil fractions were within detectable limits. If the observed soil fraction was less than the minimal fraction of soil necessary to be detectable, soil is not considered to be present. The fractions are then adjusted for interpretation.

Examination of the temporal changes in the fractions shows some interesting trends (Figure 4). For example, a distinct increase in the NPV fraction was observed in the forested wetland from June to October. This is probably due to the increasing fraction of bark and stems as the deciduous trees in the forested wetland drop their leaves. The chaparral and grasslands also show the trend toward increasing NPV as well as having detectable soil fractions in June. This trend in the chaparral may be explained by leaf drop in September and October, which increased exposure of the bark and stems while fallen leaves obscured the soil that had been visible through the canopy in June. The same trend observed in the grassland was most likely caused by other processes. Here,

the grass had senesced but was still standing upright in June; allowing some soil to be observed. Later, the grass began to fall over thereby reducing exposure of the soil.

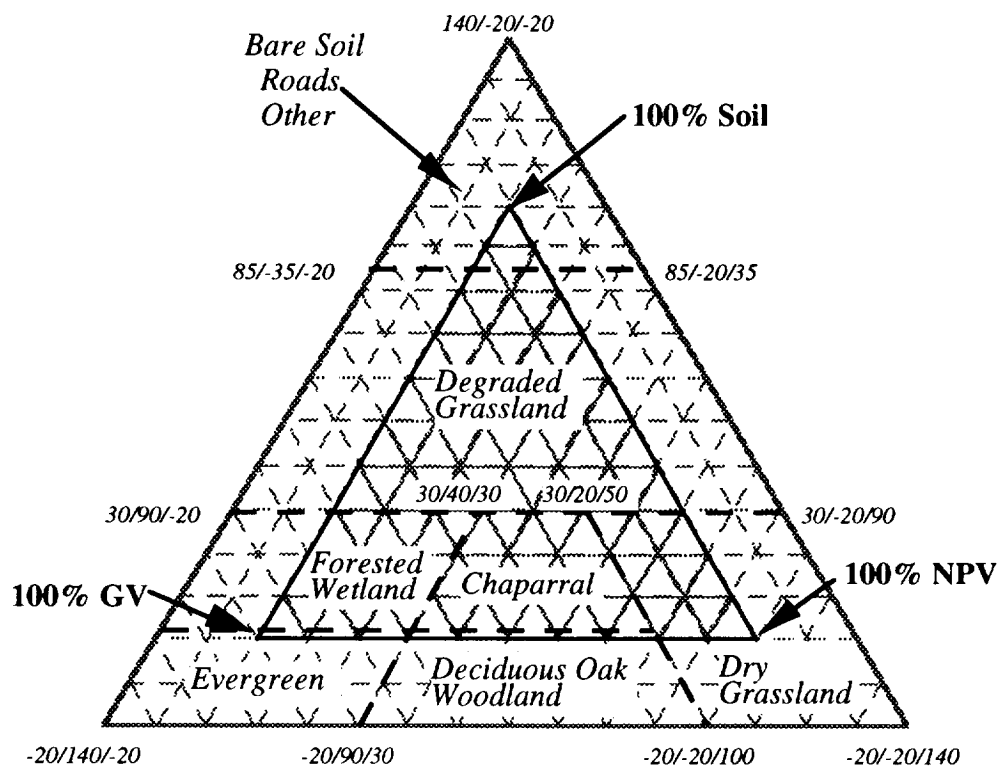


Figure 2: Ternary classification diagram used to classify the Jasper Ridge images.

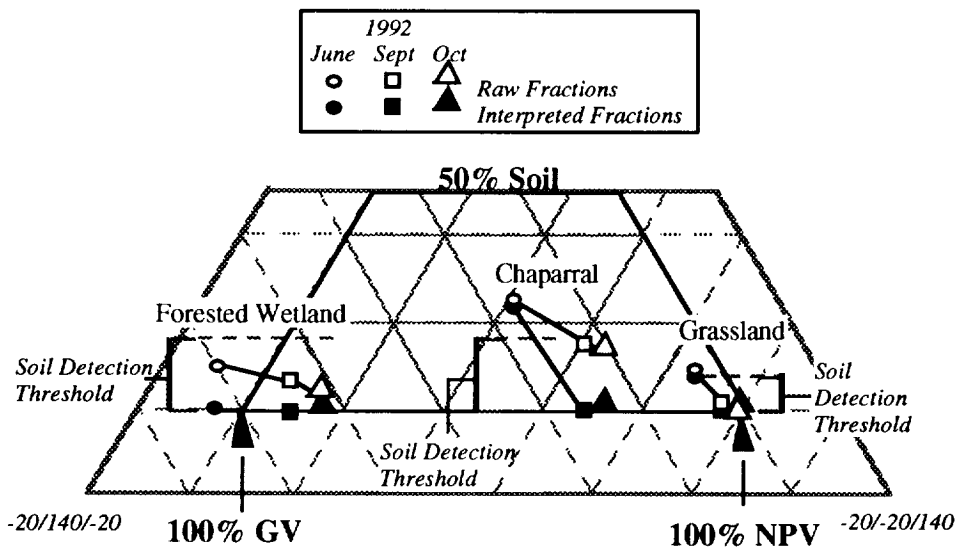


Figure 4: Temporal changes in fractions of three different plant communities of Jasper Ridge. Fractions plotted are of representative pixels representative of each community.

These seasonal trends were only observed over a part of the year, and, in the case of the grasslands, most of the growing season was missed. With the addition of image data from March or April, a more complete map of seasonal fractional variability may be produced and related to the seasonal growing cycle of various vegetational communities. With higher temporal resolution, these seasonal changes can be incorporated into the classification scheme as a way to separate spectrally similar communities with different growing cycles.

Conclusions:

- 1) Spectral mixture analysis provides a consistent framework for image interpretation, thereby allowing image classification based upon spectral fractions as well as observation of temporal changes.
- 2) Because the shade fraction is an important factor in classification of vegetational communities, it is necessary to separate the shade fraction caused by topographic effects from that caused by surface texture (for example, differential shading and shadows caused by various plant communities).
- 3) This classification scheme has yielded encouraging results in a variety of heavily vegetated images, including TM images of Brazil, MSS and TM images of northern California, and AVIRIS images of Jasper Ridge.
- 4) A clear understanding of the spectral changes in vegetation communities throughout the growing season may aid identifying spectrally similar communities with different growing cycles
- 5) Long term monitoring of any given area will allow separation of seasonal changes from longer term changes that may indicate a long-term cyclic (or permanent) changes in surface composition.

References:

- Adams, J.B., Sabol, D.E., Kapos, V., Almeida Filho, R., Roberts, D.A., Smith, M.O., and Gillespie, A.R., in preparation, Classification of multispectral images based on fractions of endmembers: Application to land-use change in the Brazilian Amazon, to be submitted to Remote Sensing of Environment.
- Gillespie, A.R., Smith, M.O., Adams, J.B., Willis, S.C., Fischer, A.F. III, and Sabol, D.E., 1990, Interpretation of residual images: Spectral mixture analysis of AVIRIS images, Owens Valley, California, Proc. Second Visible/Infrared Imaging Spectrometer (AVIRIS) Workshop. JPL Pub. 90-54, 243-270.
- Green, R.O., Conel, J.E., and Roberts, D.A., 1993, Estimation of aerosol optical depth and calculation of apparent reflectance from radiance measured by the Airborne Visible Infrared Imaging Spectrometer (AVIRIS) using MODTRAN2a, Proc. Forth Annual Airborne Geosci. (AVIRIS) Workshop, this issue.
- Ridd, M.K., Ritter, N.D., Byrant, N.A., and Green, R.O., 1992, AVIRIS data and neural networks applied to an urban ecosystem, Proc. Third Annual Airborne Geosci. (AVIRIS) Workshop. JPL Pub. 92-14, vol. 1, 129-131.
- Roberts, D.A., Smith, M.O., Adams, J.B., Sabol, D.E., and Gillespie, A.R., 1990, Isolating woody plant material and senescent vegetation from green vegetation in AVIRIS data, Proc. Second Visible/Infrared Imaging Spectrometer (AVIRIS) Workshop. JPL Pub. 90-54, 42-57.
- Roberts, D.A., Smith, M.O., Sabol, D.E., Adams, J.B., and Ustin, S., 1992, Mapping the spectral variability in photosynthetic and non-photosynthetic vegetation, soils, and shade using AVIRIS, Proc. Third Annual Airborne Geosci. (AVIRIS) Workshop. JPL Pub. 92-14, vol. 1, 38-40.
- Sabol, D.E., Adams, J.B., and Smith, M.O., 1992a, Quantitative subpixel spectral detection of targets in multispectral images, J. Geophys. Res. 97, 2659-2672.
- Sabol, D.E., Roberts, D.A., Smith, M.O., and Adams, J.B., 1992b, Temporal variation in spectral detection thresholds of substrate and vegetation in AVIRIS images, Proc. Third Annual Airborne Geosci. (AVIRIS) Workshop. JPL Pub. 92-14, vol. 1, 132-134.